Magnetic Resonance in Medicine 43:34–44 (2000)

# A Model of Unloaded Human Intervertebral Disk Based on NMR Relaxation

Teresa Nightingale,[1] Alex MacKay,[1,2]* Richard H. Pearce,[3] Kenneth P. Whittall,[2] and Borys Flak[2]

**NMR relaxation rates were related to the composition of the nucleus pulposus from 11 and anulus fibrosus from six human intervertebral disks. Tissue water was proportional to glycosaminoglycan (GAG) and residue, the noncollagen, non-GAG portion of the dry weight ($R^2 = 0.74$). The solid signal fraction depended on collagen and residue protons ($R^2 = 0.89$). $1/T_1$ was proportional to collagen and residue ($R^2 = 0.97$). $T_2$ showed 2–4 components labeled A, B, C, and D, with means ± standard deviations of 3.1 ± 1.6, 17.5 ± 9.5, 64 ± 22, and 347 ± 162 msec. Signal fractions of A and B depended on the collagen-associated water protons ($R^2 = 0.94$ and 0.85), C on residue-associated water protons ($R^2 = 0.82$), and D on GAG-associated water protons ($R^2 = 0.74$). The data led to a model of disk architecture in which the collagen and residue were largely solid, forming distinct water compartments; the remaining water was present in a proteoglycan gel. Magn Reson Med 43:34–44, 2000.** © **2000 Wiley-Liss, Inc.**

**Key words: NMR; intervertebral disk; collagen; glycosaminoglycan**

Intervertebral disk degeneration is generally believed to play a central role in the pathogenesis of low back pain and is thus responsible for much human suffering and substantial health care costs. The healthy young intervertebral disk comprises a coarsely fibrous ring, the anulus fibrosus (AF), surrounding a centrally located translucent nucleus pulposus (NP). The NP is bounded above and below by end plates consisting of a thin hyaline cartilage overlaying compact bone on the ends of the vertebrae. With age, the NP becomes a fibrous pad that eventually develops fine fissures, and later clefts, that in extreme cases may separate the NP entirely from the surrounding tissue. The distinction between the NP and AF becomes less clear with age and clefts may develop within the AF (1).

Aging and degeneration of the disk are associated with changes in the concentrations of its chemical constituents (2,3). The predominant chemical constituents are water, collagen, proteoglycan, and non-collagenous, non-proteoglycan proteins. Water content decreases markedly from birth to maturity, more slowly from maturity until death, and more prominently in the NP than in the AF. More collagen is present in the AF than in the NP; the NP collagen increases with aging and degeneration. Proteoglycan is more abundant in the NP than in the AF, and in the NP its concentration decreases with aging and degeneration.

MRI is an important noninvasive clinical method for documenting the state of the intervertebral disk (4,5). Several groups related tissue composition to the NMR properties of the disk. $1/T_1$ was related linearly to the water concentration in disks (6). Two other groups (7,8) plotted $T_1$ versus water concentration and found an apparently hyperbolic relationship, suggesting that water concentration is more likely linearly related to $1/T_1$ rather than to $T_1$. A study (7) that related $T_1$ to nonaqueous components of disk found $T_1$ to be positively correlated to GAG and negatively correlated to collagen concentrations. Although one study found that $T_2$ decay curves from rabbit spine were multi-exponential (9), all other studies of $T_2$ in disks used single exponential analyses. Several groups examined the correlation between $1/T_2$ and water concentration; Ke et al. (10) found very good correlation, Weidenbaum et al. (11) found marginal correlation, and Chiu et al. (12) found none. Two groups (6,7) found reasonable linear correlations between $T_2$ and water concentration, while Chatani et al. (8) demonstrated a curvilinear plot for $T_2$ versus water concentration. Antoniou et al. (7) and Majors et al. (6) found positive correlations between $T_2$ and GAG concentration, whereas Weidenbaum et al. (11) found no correlation between $1/T_2$ and GAG concentration. Antoniou et al. (7) and Majors et al. (6) found negative correlations between $T_2$ and collagen concentration, whereas Weidenbaum et al. (11) found a positive correlation between $1/T_2$ and collagen. In short, the literature relating chemical composition to the NMR properties of the disk is inconclusive.

This investigation develops a model of the architecture of the human lumbar disk based on the effect of chemical composition on its NMR properties. The approach differs from most other disk studies. The NMR spectrometer was sensitive to all protons in the disk, not just to the mobile protons accessible to a clinical MRI scanner. Special effort was made to look for multi-component $T_1$ and $T_2$ relaxation behavior. Assays of the principal chemical constituents—water, collagen, and proteoglycan—used methods that could be related directly to the weight of the constituents. This study looked for correlations between NMR and chemical composition that were not only statistically significant, but also had a plausible NMR interpretation.

## MATERIALS AND METHODS

### Collection of Specimens

Lumbar disk samples were obtained from human spines collected within 24 h of death. A mid-sagittal $T_2$-weighted

[1]Department of Physics, Faculty of Science, University of British Columbia, Vancouver, Canada.

[2]Department of Diagnostic Radiology, Faculty of Medicine, University of British Columbia, Vancouver, Canada.

[3]Department of Pathology, Faculty of Medicine, University of British Columbia, Vancouver, Canada.

*Correspondence to: Alex MacKay, Department of Physics and Astronomy, University of British Columbia, 6224 Agricultural Road, Vancouver, BC, Canada V6T 1Z1. E-mail: mackay@physics.ubc.ca

Received 16 September 1998; revised 30 August 1999; accepted 3 September 1999.

image ($T_R$ – 2000 msec; $T_E$ – 40 msec) was made within 4 h of specimen collection using a 0.15-T Picker Vista MRI Scanner. To evaluate degeneration (13), each disk image was graded independently and blindly by a radiologist (BF) experienced with the grading scheme. The grades ranged from healthy young grade I to severely degenerate grade V. Specimens were frozen quickly and stored at −80°C. Before dissection, the spine was thawed overnight at 4°C.

Intervertebral disks of known grade were dissected, taking care to avoid inclusion of the cartilaginous end plate. NP, that is, centrally-located tissue free of coarse collagenous fiber bundles, and AF, that is, peripherally-located tissue comprising coarse collagenous fiber bundles through the full thickness of the disk, were dissected. Blocks of tissue weighing approximately 0.2 g were placed without compression into 8 mm diameter NMR tubes and sealed. Dissected tissue samples were stored at −30°C and thawed to room temperature only for NMR measurements. Refreezing and rethawing did not affect the NMR results, in agreement with other work (Thompson, Master's thesis, University of British Columbia). Since AF samples exhibited some angular dependence in the NMR free induction decay, the samples were oriented with fibers perpendicular to the magnetic field at which orientation the free induction decay rate was found to be slowest.

## Collection of NMR Data

Proton NMR data were collected on a modified Bruker 2.1-Tesla solid-state spectrometer (14) capable of characterizing the signal from all protons in disk samples. The magnetic field homogeneity was about 0.5 ppm and all measurements were made at 24° with a repetition time of 10 sec; 100 signals were averaged.

The free induction decay was measured following a 90° pulse. To minimize coherent noise and baseline offsets, alternate 90° pulses were preceded 1 msec earlier by a 180° pulse to invert the signal, which was subtracted from the cumulative signal averaged data. Signals from both x and y channels were collected to permit correction of any phase offsets. A dwell time of 0.5 μs was used and 1024 points were digitized. For the first 12 μs following the center of the 90° pulse, the signal was distorted due to receiver saturation. Protons that were either rigid or underwent anisotropic motion on the NMR time scale of $10^{-5}$ sec contributed to the ''solid'' signal; such signals decayed to zero in less than 50 μs. The total signal, S(t), from 12 to 20 μs was fitted to the equation (15)

$$S(t) = S(0)\left(1 - \frac{M_2}{2}t^2\right), \qquad [1]$$

where $M_2$ is the second moment of the proton NMR line shape. Assuming that the mobile signal has zero $M_2$, the $M_2$ of the protons in tissue solids was $\sim 3 \times 10^9$ $s^{-2}$ for all samples. The mobile signal from protons that undergo rapid isotropic motion on the NMR time scale decayed much more slowly and was characterized by

$$S(t) = M(0)\, e^{-t/T_2} \qquad [2]$$

for times greater than 50 μs. The fraction of the signal from the solid protons was (S(0) – M(0))/S(0) while that from the mobile signal was M(0)/S(0).

Spin-lattice relaxation was measured using the same pulse sequence as the free induction decay, but the inversion time between the 180° and the 90° pulse was varied for 11 intervals logarithmically spaced between 1 msec and 5 sec. To obtain the $T_1$ decay curve, the average of a small data window in the free induction decay signal immediately following the receiver saturation time (12 μs) was plotted against inversion time. The $T_1$ decay curve had contributions from both solid and mobile protons.

The Carr-Purcell-Meiboom-Gill (CPMG) (16,17) sequence was used for $T_2$ measurement. To minimize coherent noise and baseline offset, on alternate scans the phase of the 90° pulse was shifted by 180° and the signal alternately added and subtracted from the computer memory. For a few samples, results were acquired at echo spacings, τ, of 200, 400, and 800 μs to look for dependence of the $T_2$ decay curves upon τ. No dependence was found, permitting subsequent data collection to be restricted to τ times of 200 and 400 μs. In all cases but one, the 200 and 400 μs results were identical. Results presented here are for the 200 μs echo spacing only. For $T_2$ decay curves, four points were averaged from each echo for the first 224 echoes and four points were averaged from every eighth echo for the next 512 echoes. $T_2$ decay curves were terminated when their amplitude had decayed to 1% of the initial amplitude.

$T_1$ and $T_2$ decay curves were fitted by the expression

$$S(t) = \sum_{i=1,N} S_i(0)\, e^{-t/T_{j,i}} \qquad [3]$$

for $j = 1, 2$, where $S(t)$ is the $T_1$ or $T_2$ decay curve amplitude at time $t$, $N$ is the number of exponential components, and $S_i(0)$ and $T_{j,i}$ are the initial amplitude and the $T_1$ or $T_2$ time of the $i^{th}$ component. The above equation was fitted using a Non-Negative-Least-Squares (NNLS) algorithm (18). The closeness of the fit to the data was monitored by calculation of $\chi^2$ and by plotting the fitted curve. For most samples, $\chi^2$ was between 0.9 and 1.2 times the number of data points. In all cases, there was excellent agreement between the data and the fitted curve.

## Chemical Composition of the Tissue

After NMR, the tissue was minced finely and duplicate samples were taken for analysis. Water content of the tissue samples was measured as the weight lost on freeze-drying followed by further drying in vacuo to constant weight over $P_2O_5$ (19). Samples were digested with papain and the digest was assayed for hydroxyproline (20) and for anion-exchanger-bound hexose and hexuronate (21). All concentrations were expressed relative to the dry weight of the tissue because of postmortem shifts of tissue water (22). Collagen concentration was calculated using the factor 0.91 g collagen/mmol hydroxyproline (19), keratan sulfate concentration using the factor 0.495 g keratan sulfate/mmol galactose, and chondroitin sulfate concentration using the factor 0.503 g chondroitin sulfate/mmol Na glucuronate. Keratan sulfate and chondroitin sulfate values were summed to obtain the total glycosaminoglycan

(GAG) concentration. Residue was dry weight less collagen and GAG.

### Preparation of 4 M Guanidinium Chloride-Insoluble Tissue Solids and Proteoglycan

Tissue solids, which comprised mainly collagen, and proteoglycan were prepared from NP or AF from tissues other than those used for NMR studies in order to examine the NMR properties of individual tissue constituents. The A1 proteoglycan was extracted with buffered 4M guanidinium chloride containing protease inhibitors followed by CsCl density gradient ultracentrifugation, as described elsewhere (23). The tissue solids remaining after extraction with 4M guanidinium chloride were washed thoroughly with buffered physiological saline and stored as a thick slurry (23).

### Statistical Treatment of Data

The data were analyzed using Systat for Windows, Version 5.03. Because the data were generally not distributed normally, comparisons of two groups used the Mann-Whitney U-test. Analysis of variance was used to examine the differences among the four components in $\log_{10} T_2$; Scheffé's test was used to evaluate differences between components. The closeness of fit to a linear regression was evaluated using the coefficient of correlation squared ($R^2$), which expresses the fraction of the variance of the dependent variable attributable to the regression, and the standard error of estimate. The significance of $R^2$ was evaluated by the F-test. Initially, the effects of collagen, GAG, and residue concentrations were tested using a mixture model because these components summed to the dry weight, a constant. Nonsignificant variables were eliminated and the linear regression analysis was repeated with the remaining variables until all nonsignificant variables had been eliminated. Because the three variables were not independent, any pair gave identical values of $R^2$. In such cases, the variables relating positively to relaxation rates were used because such relationships are more plausible physically (24). For each such relationship reported, the effect of correlations amongst the independent variables was examined as well as the normality of the distributions of residuals about the line of best fit and the effect of outliers on the coefficients.

## RESULTS

Disks for study were selected by the appearance of their $T_2$-weighted spin-echo images ($T_R$ – 2000 msec; $T_E$ – 40 msec) using the grading scheme of Thompson et al. (13). Eleven disks from ten donors were used, one of grade I, four of grade II, four of grade III, and two of grade IV. Disks of grades I and II were considered healthy; those of grades III and IV, degenerate. Five donors of healthy disks ranged in age from 17 to 42 y; six donors of degenerate disks, from 24 to 85 y. Nine of the ten donors were male. NP from each of the disks and AF from six were used for experiments.

### Tissue Composition Was Typical of Human Disks

After completion of NMR measurements, 13 specimens were analyzed for water, collagen, and GAG. Results were typical of human intervertebral disks analyzed in this laboratory. Two specimens with outlying values were excluded from subsequent analyses in which the concentrations of tissue components were compared with NMR parameters. These two samples appeared to have degraded during storage because of poorly sealed NMR tubes. The mean water concentration (± SD) of the NP (2.74 ± 0.64 g/g dry wt) was higher ($P = 0.021$) than that of the AF (1.84 ± 0.38 g/g). The mean collagen concentration was higher ($P = 0.013$) in the AF (0.64 ± 0.11 g/g) than in the NP (0.31 ± 0.09 g/g). The mean GAG concentration was higher ($P = 0.03$) in healthy NP (0.45 ± 0.11 g/g) than in degenerate NP (0.20 ± 0.13 g/g). The mean concentration of the residue (dry wt less collagen and GAG) was 0.34 ± 0.20 g/g dry wt and did not differ significantly between NP and AF or between healthy and degenerate NP.

### Water Concentration Depended on GAG and Residue Concentrations

GAG, collagen, and residue concentrations were fitted to an equation expressing water concentration as a linear function of these three variables by using a mixture model. GAG ($P < 0.001$) and residue ($P < 0.001$) contributed significantly to the regression, but collagen did not ($P = 0.52$):

$$\text{WATER} = 0.39\ (\pm 0.57)\ \text{COLLAGEN} + 5.28\ (\pm 0.60)\ \text{GAG} + 2.59\ (\pm 0.45)\ \text{RESIDUE}. \quad [4]$$

The water concentration in the collagen compartment, 0.39 ± 0.59 g/g collagen ($P = 0.40$), was much less than that in the residue and GAG compartments, 2.59 ± 0.45 g/g residue ($P = 0.002$) and 5.28 ± 0.60 g/g GAG ($P < 0.001$), respectively. Water concentration calculated using this equation agreed well with observed values (Fig. 1) . Thus, the water concentration in the tissue depended on the concentrations of GAG and residue. Because of these relationships, water was not treated as an independent variable; rather, collagen, GAG, and residue were treated as distinct water compartments.

### Water Protons Predominate in Tissue

The proton concentration in water is 0.111 g proton/g. The numbers of nonexchangeable protons of collagen, keratan sulfate, and chondroitin sulfate were calculated by counting the –CH bonds of the constituent amino acids of human NP collagen (25) and of the disaccharide repeating units of the two GAGs. Protons covalently bound to oxygen, nitrogen, or sulfur were assumed to exchange sufficiently rapidly to be indistinguishable from those of water (26). Calculated densities were 0.0460, 0.0343, and 0.0301 g proton/g of NP collagen, keratan sulfate, and chondroitin sulfate, respectively. Residue, the other component, was assumed to have a proton density of 0.04 g proton/g dry wt. These values were used to calculate the fractions of the tissue protons associated with water, collagen, GAG, and residue in each tissue sample. Mean values (± SD) were 0.868 ± 0.037, 0.058 ± 0.037, 0.027 ± 0.013, and 0.046 ±

0.028 for water, collagen, GAG, and residue, respectively. The water protons predominated. Collagen, GAG, and residue protons contributed about 13% to the tissue protons.

### Collagen and Residue Are Solids

Free induction decay (FID) curves from typical healthy NP and AF are shown in Fig. 2. The initial rapidly-decaying FID component arises from protons on molecules that move slowly or anisotropically on the NMR time scale of $10^{-5}$ sec. Collagen is an obvious candidate for this solid component. A higher proportion of collagen is present in the AF than in the NP, and the rapid decay was more prominent in the AF than in NP. Also, the 4M guanidinium chloride-insoluble solids, which contain the bulk of the disk collagen, showed a rapidly decaying component of the free induction decay signal similar to that shown by disk tissues. Solutions of disk A1 proteoglycan in phosphate-buffered saline did not. However, the dependence of the solid signal on the fraction of collagen protons was weak, accounting for only 46% ($R^2$) of the variance in the solid signal ($P = 0.14$) with a standard error of estimate of 0.038. On the other hand, the solid component of the signal corresponded closely to the sum of the proton fractions of collagen and residue (Fig. 3a):

$$\text{SOLID FRACTION} = -0.018\ (\pm 0.018) + 0.82\ (\pm 0.15) \cdot \text{PROTON FRACTION (collagen + residue)}. \quad [5]$$

The solid signal fraction was consistently less than the sum of the proton fractions of collagen and residue by $0.039 \pm 0.016$, suggesting that some residue or collagen contributed to the mobile signal.

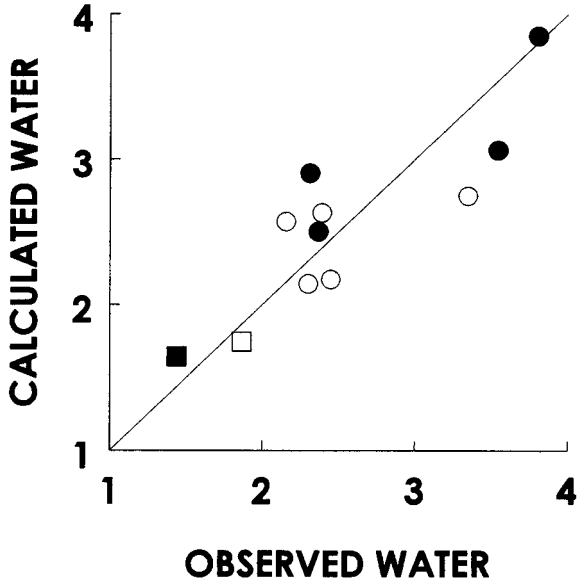


FIG. 1. Observed concentration of water (g/g dry wt) in healthy (●,■) and degenerate (○,□) nucleus pulposus (●,○) and anulus fibrosus (■,□) compared with values calculated by the equation WATER = 0.39 COLLAGEN + 5.28 GAG + 2.59 RESIDUE. The line corresponds to equal values. $R^2 = 0.74$; $P = 0.004$. Standard error of estimate = 0.41g water/g dry wt.

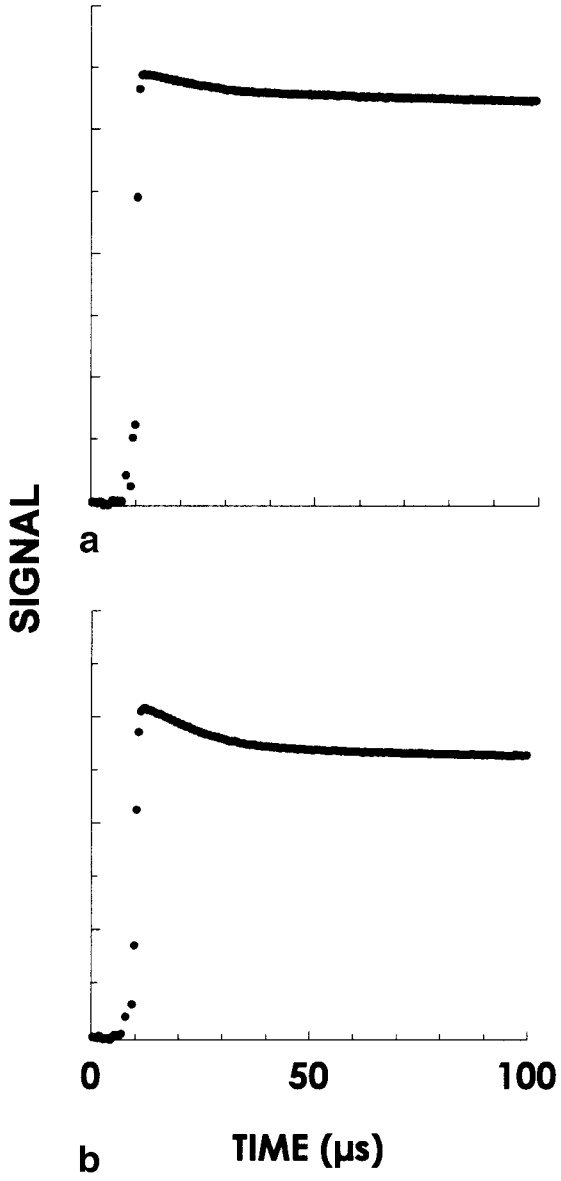


FIG. 2. Typical free induction-decay curves of (**a**) nucleus pulposus and (**b**) anulus fibrosus.

### Water and GAG Are Mobile

Since the tissue fresh weight is the sum of water, collagen, GAG, and residue, a corollary of the relation of collagen and residue to the solid signal is the relation of water and GAG to the mobile signal (Fig. 3b):

$$\text{MOBILE FRACTION} = 0.19\ (\pm 0.13) + 0.82\ (\pm 0.15) \cdot \text{PROTON FRACTION (water + GAG)}. \quad [6]$$

Water alone accounted for 69% of the variance of the mobile fraction. The relationship of water and GAG to the mobile signal is supported by the demonstration that the water content of the disk depends upon the fixed charge density of the tissue GAG (27).

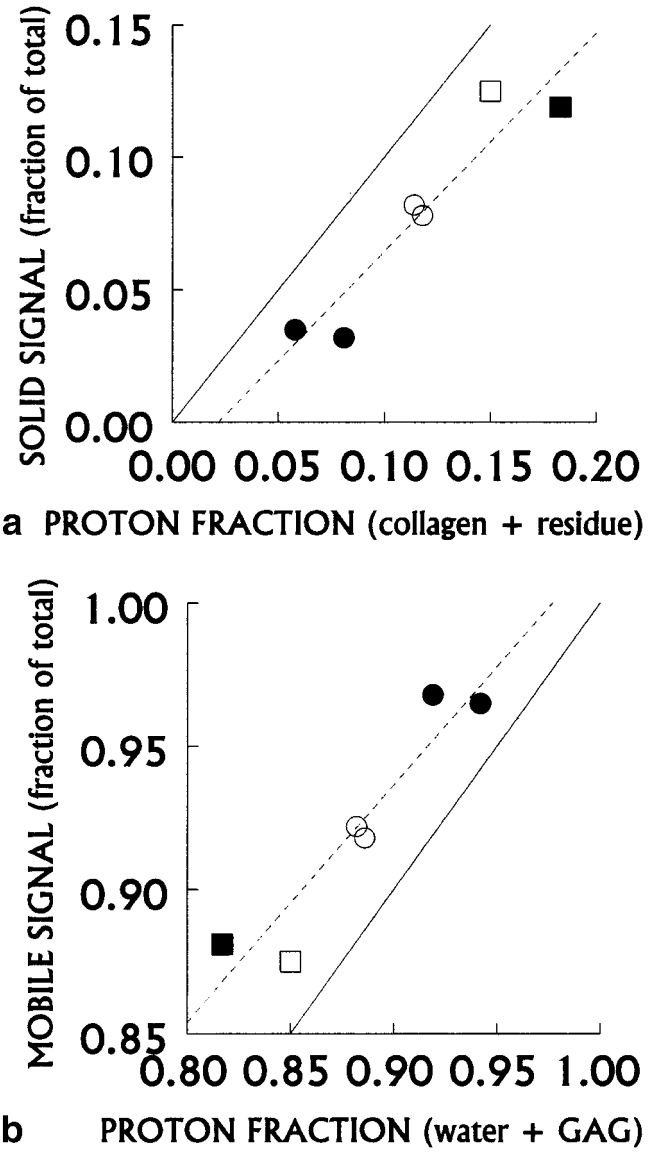


FIG. 3. Free induction-decay signals compared with proton fractions calculated from tissue components of healthy (●,■) and degenerate (○,□) nucleus pulposus (●,○) and anulus fibrosus (■,□). The solid lines represent agreement between the signal fraction and the proton fraction. The dashed lines represent the lines of best fit. **a:** The solid signal compared with collagen plus residue. $R^2 = 0.89$; $P = 0.005$. Standard error of estimate = 0.038. **b:** The mobile signal compared with water plus GAG. $R^2 = 0.89$; $P = 0.005$. Standard error of estimate = 0.015.

### $1/T_1$ Was Related to Collagen and Residue Concentrations

$T_1$ relaxation curves followed a single component exponential decay. Therefore, on the $T_1$ time scale of about 1 sec, all solid and mobile protons are in equilibrium. All the $T_1$ rates for tissues were higher than those found for 4M guanidinium chloride-insoluble tissue solids or A1 proteoglycan preparations.

The relationship of $1/T_1$ to collagen, GAG, and residue concentrations was calculated using a mixture model. The contributions of collagen and residue were significant ($P < 0.001$ for both) whereas the contribution of the GAG was not ($P = 0.50$). Thus, the $T_1$ relaxation rate is a linear function of collagen and residue concentrations:

$$1/T_1 = -0.18\ (\pm 0.13) + 1.89\ (\pm 0.18) \cdot \text{COLLAGEN} + 1.72\ (\pm 0.18)\ \text{RESIDUE}. \quad [7]$$

The observed values fitted the calculated values well (Fig. 4). This relationship supports a fast exchange model in which water protons, which dominate the disk signal, are relaxed by interactions with collagen and residue molecules (24).

### $T_2$ Relaxation Was Multi-Component

A typical $T_2$ decay curve obtained from the CPMG sequence is shown in Fig. 5. The curvature of the semilogarithmic plot indicated a departure from the simple exponential decay characteristic of a single water environment. A NNLS fit indicated four $T_2$ water environments (Fig. 5, inset); each characterized by a time constant, $T_{2X}$, and a fraction of the total signal. Similar analyses of the 17 specimens identified two to four components: two for four specimens, three for seven, and four for six. For the six specimens with four components, the mean values ± SD were 3.1 ± 1.6, 17.5 ± 9.4, 64 ± 22 and 347 ± 162 msec. These components will be designated A, B, C, and D in order of increasing $T_{2X}$. $\text{Log}_{10}\ T_{2X}$ was used for statistical analysis because the standard deviations were proportional to the magnitude of $T_2$. The values of $\log_{10}\ T_{2X}$ differed clearly between the four components ($P < 0.001$ by analysis of variance). $T_{2X}$ for each of the components differed clearly from the others ($P < 0.001$ by Scheffé's test

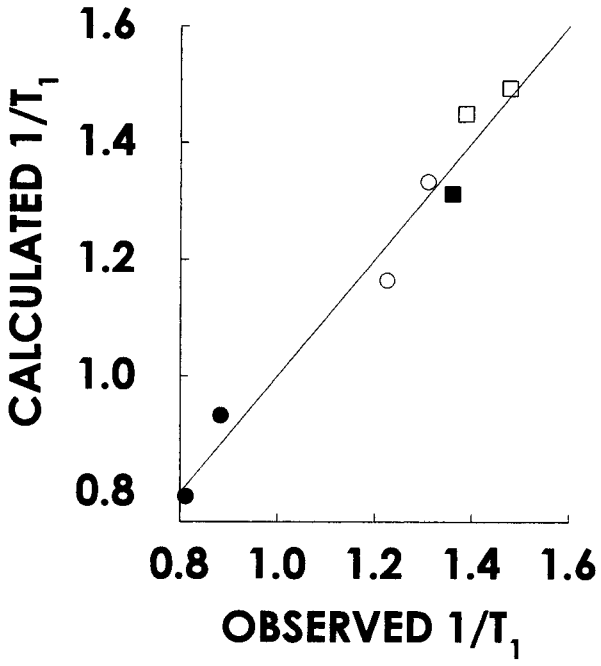


FIG. 4. The observed $T_1$ relaxation rates ($sec^{-1}$) of healthy (●,■) and degenerate (○,□) nucleus pulposus (●,○) and anulus fibrosus (■,□) compared with values calculated by the equation $1/T_1 = -0.18 + 1.89$ COLLAGEN + 1.72 RESIDUE. The line corresponds to equal observed and calculated values. $R^2 = 0.97$; $P = 0.001$. Standard error of estimate = 0.096 $sec^{-1}$.

for each pair). $T_{2X}$ for the specimens with two or three components were assigned to component A, B, C or D by calculating the probability that the value of $T_{2X}$ arose from each one of the four components using the mean and standard deviation of the values from the four-component specimens as a reference. The datum was assigned to the component with the highest probability.

### Fractions of the $T_2$ Components Depended on Disk Morphology

The fractions of $T_2$ components for the NP and AF of healthy and degenerate disks are shown in Fig. 6. Component D was absent for all samples of AF and either absent or negligible for four of the five samples of degenerate NP. In contrast, for healthy NP the fraction of component D was over 0.83 of the total signal for three of the four specimens tested and 0.49 in the fourth. The fraction of component C was over 0.89 of the total signal in four of the five degenerate NP, zero in two of the healthy NP and 0.12 and 0.31 in the remaining two. This pattern suggested that component D was characteristic of healthy NP and component C of degenerate NP. For the AF, the predominant components of the $T_2$ relaxation were B and C, with component B predominating in the degenerate AF.

### Fractions of the $T_2$ Components Depended on Tissue Constituents

In the absence of exchange, the magnitude of each $T_2$ fraction should reflect the fraction of the tissue mobile protons associated with the constituent or constituents responsible. The fraction of water protons associated with each component was calculated using the coefficients relating collagen, GAG and residue concentrations to the concentration of tissue water: 0.39 g water/g collagen, 5.29 g water/g GAG, and 2.59 g water/g residue (Eq. [4]). Collagen and residue protons were not included because they contributed mainly to the solid and not to the mobile signal. The GAG protons were also not included because they contributed on average only about 3% to the signal.

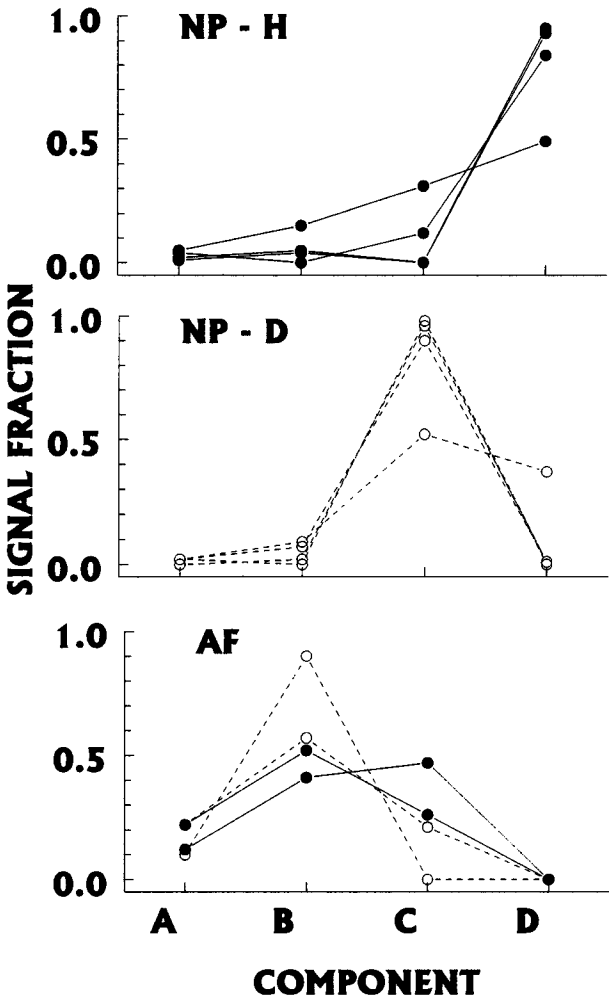


FIG. 6. The fraction of the $T_2$ components in healthy (H, ●—●) and degenerate (D, ○—○) nucleus pulposus (NP) and healthy (■—■) and degenerate (□—□) anulus fibrosus (AF). Two specimens gave identical results in panel NP – D.

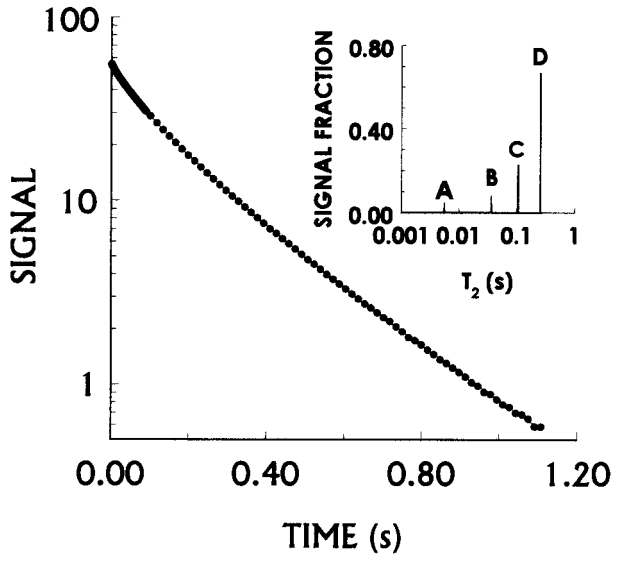


FIG. 5. A $T_2$ relaxation curve obtained for a nucleus pulposus by the Carr-Purcell-Meiboom-Gill sequence. Inset: the non-negative least squares $T_2$ distribution derived from the curve. The letters identify the components.

The dependence of the signal fraction of each of the $T_2$ components on the fractions of water in collagen, GAG and residue was examined by a mixture model of multiple regression (Table 1). Components A and B depended principally on collagen concentration, component C on residue concentration, and component D on GAG concentration. The regression of each of the components on the constituent having the principal effect was calculated (Table 1). The fraction of component A depended linearly on the collagen-associated water fraction (Fig. 7a). Some caution should be observed in drawing this conclusion since the data for NP and AF separated into two clusters. When the data for NP alone were examined, the dependence was not seen ($R^2 = 0.20$; standard error of estimate 0.013). However, since all values for NP were less than 5% of the signal, any trend may have been lost in the uncertainty of the measurements. The component B signal fraction depended linearly on the collagen-associated water fraction (Fig. 7b). This conclusion, too, should be

Table 1
The Dependence of $T_2$ Components on the Composition of the Disks

| $T_2$ component | Probability ($P$) that coefficient is zero for water associated with | | |
|---|---|---|---|
| | Collagen | GAG | Residue |
| A | <0.001 | 0.14 | 0.04 |
| B | 0.004 | 0.55 | 0.63 |
| C | 0.55 | 0.70 | <0.001 |
| D | 0.26 | 0.001 | 0.36 |

*The fraction of each $T_2$ component was fitted to a mixture model of linear regression. The probability that each coefficient was zero was calculated. For the highly significant coefficients, the linear regression of the component fraction on the fraction of constituent-associated water was calculated. The fitted equations were as follows:

$$\text{COMPONENT A} = -0.025\ (\pm 0.008) + 1.09\ (\pm 0.09)\ \text{COLLAGEN FRACTION} \quad [8]$$

$$\text{COMPONENT B} = -0.085\ (\pm 0.026) + 3.10\ (\pm 0.30)\ \text{COLLAGEN FRACTION} \quad [9]$$

$$\text{COMPONENT C} = -0.114\ (\pm 0.108) + 1.77\ (\pm 0.27)\ \text{RESIDUE FRACTION} \quad [10]$$

$$\text{COMPONENT D} = -0.55\ (\pm 0.29) + 1.65\ (\pm 0.44)\ \text{GAG FRACTION.} \quad [11]$$

accepted cautiously because of the separation of the data into NP and AF clusters and the loss of significance when data for NP alone were considered ($R^2 = 0.21$). The component C fraction related linearly to the residue-associated water fraction (Fig.7c). The values for healthy and degenerate specimens of NP and AF were distributed over the range of both variables, lending confidence in the general applicability of the relationship. The component D fraction related linearly to the GAG water fraction (Fig. 7d). The calculated regression was influenced strongly by the large number of zero values. The data for healthy NP alone were not significant ($P = 0.30$). The data of Fig. 7d suggested a sigmoid relationship between component D fraction and GAG-associated water. The transition occurred between GAG-associated water fractions of 0.55 and 0.8, suggesting that in these unloaded disks when the GAG-associated water protons were below 55%, GAG was unable to maintain a distinct water environment. The predominance of component D in healthy NP and of component C in degenerate NP suggested that degeneration involved the movement of water from the GAG compartment to the residue compartment. With the possible exception of component A, the signal fraction did not match the relevant water fraction suggesting that the relationship between the mobile signal and the constituent-associated water was more complex.

The uncertainty of the coefficients relating water to each tissue constituent, particularly collagen, lent uncertainty to the relationships of the four water compartments to the tissue constituents as described above. Therefore, the relationships of the $T_2$ signal fractions to the weight concentrations of tissue collagen, GAG and residue were calculated as well. The fraction of the variance of the signal accounted for by the concentrations of the constituents ($R^2$) followed the pattern found when the concentration of constituent-associated water was used. However, the $R^2$ values were somewhat lower: 0.78 for fraction A and collagen ($P < 0.001$), 0.57 for fraction B and collagen ($P = 0.004$), 0.75 for fraction C and residue ($P = 0.001$), and 0.87 for fraction D and GAG ($P < 0.001$). This result supports our hypothesis that the $T_2$ component fractions are related more closely to the water associated with the tissue constituents than to the weights of the constituents.

## $T_2$ Relaxation Rates Relate to Collagen and Residue Concentrations

In the absence of exchange effects, the relaxation rates of each of the four compartments should reflect the environment of the associated protons. This hypothesis was tested by an examination of the combined effects of collagen, GAG, and residue on each of the four $T_2$ relaxation rates. The proportions of the variances in rate attributable to all three constituents ($R^2$) were 12%, 59% ($P = 0.07$), 14%, and 41% for components A, B, C, and D, respectively. Only the data for component B suggested a possibly significant relationship. The four $T_2$ relaxation rates of the tissues were all faster than those seen for the 4M guanidinium chloride-insoluble tissue solids or for purified disk A1 proteoglycan.

The relaxation rate of $T_2$ component B was proportional to the concentration of the residue in NP only (Fig. 8). The line of best fit was

$$1/T_{2B} = 41.7\ (\pm 4.2) + 94.5\ (\pm 10.9)\ \text{RESIDUE.} \quad [12]$$

The data for AF did not fall on the line. The water protons associated with component B, the relative size of which was determined by the tissue collagen concentration (Eq. [9]), relaxed in the NP at a rate determined by the concentration of the residue.

Components C and D, the relative sizes of which were determined by the GAG and residue concentrations (Eqs. [10] and [11]), respectively, represent the bulk of the signal from NP. Therefore, the mean relaxation rate of these two components, weighted by their fraction in the signal, corresponds to the signal measured by contemporary clinical scanners. An examination of the effects of collagen, GAG, and residue concentrations on this relaxation rate (Fig. 9) revealed that both collagen and residue affected the variance significantly ($P < 0.001$ for both):

$$1/T_{2CD} = -11.3\ (\pm 4.2) + 41.4\ (\pm 6.7)\ \text{COLLAGEN} + 36.7\ (\pm 5.8)\ \text{RESIDUE.} \quad [13]$$

The bulk of the water protons appeared to occupy an environment in which the $T_2$ properties were dominated by collagen and residue. Thus, even though GAG is responsible for the shift of water from component D to component C during degeneration, the role of GAG in determining the NMR relaxation rate was negligible.

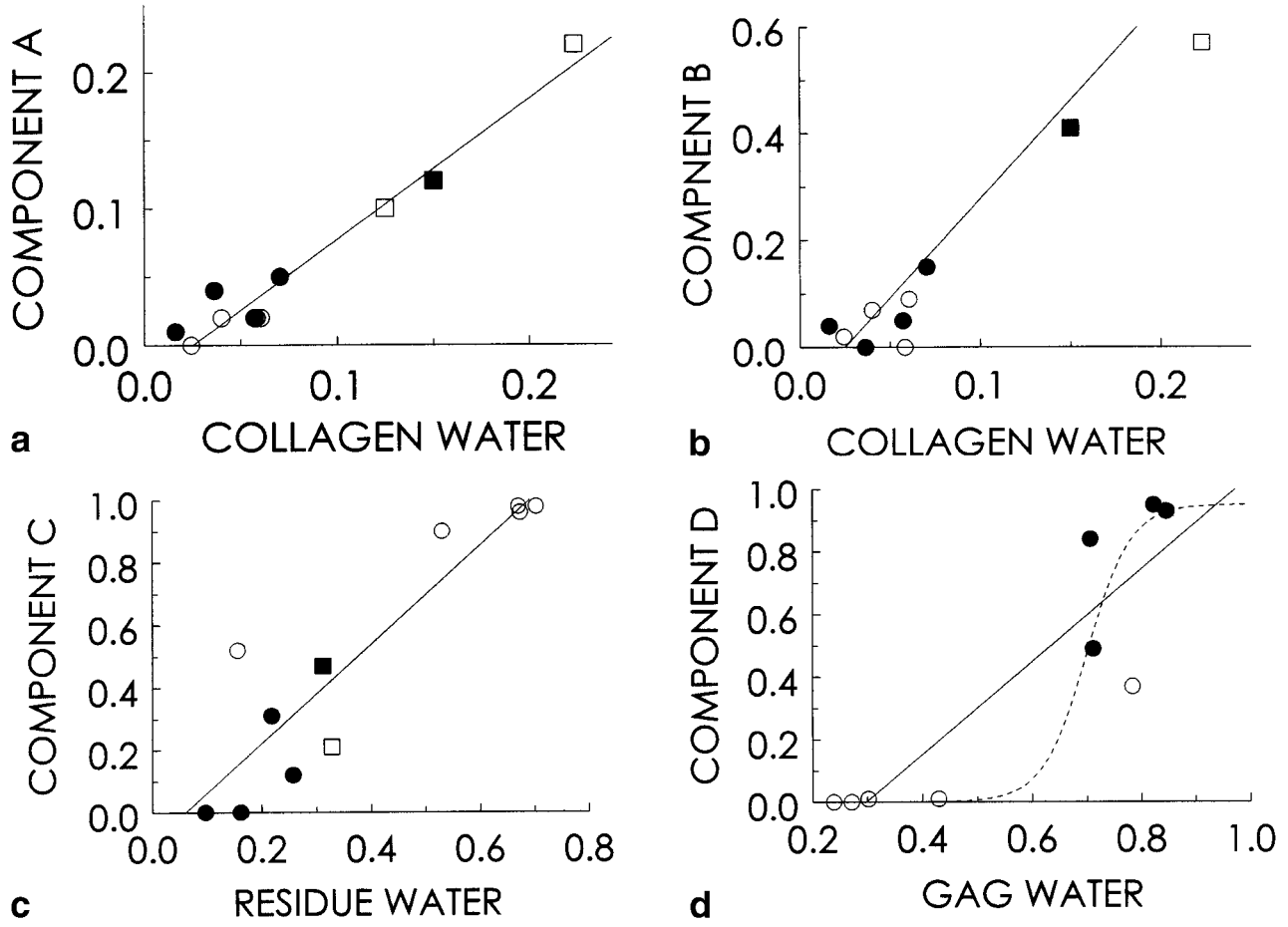


FIG. 7. The effect of constituent water fractions on the $T_2$ component fractions of healthy (●,■) and degenerate (○,□) nucleus pulposus (●,○) and anulus fibrosus (■,□). The lines of best fit are shown. **a:** The effect of collagen water on component A. $R^2 = 0.94$; P<0.001. Standard error of estimate = 0.016. **b:** The effect of collagen water on component B. $R^2 = 0.85$; $P < 0.001$. Standard error of estimate = 0.055. **c:** The effect of residue water on component C. $R^2 = 0.82$; $P < 0.001$. Standard error of estimate = 0.18. **d:** The effect of glycosaminoglycan (GAG) water on component D. $R^2 = 0.74$; $P = 0.013$. Standard error of estimate = 0.23. The dashed line was calculated using the equation: Component D = $0.95/(1 + e^{-25/(\text{GAG water} - 0.7)})$.

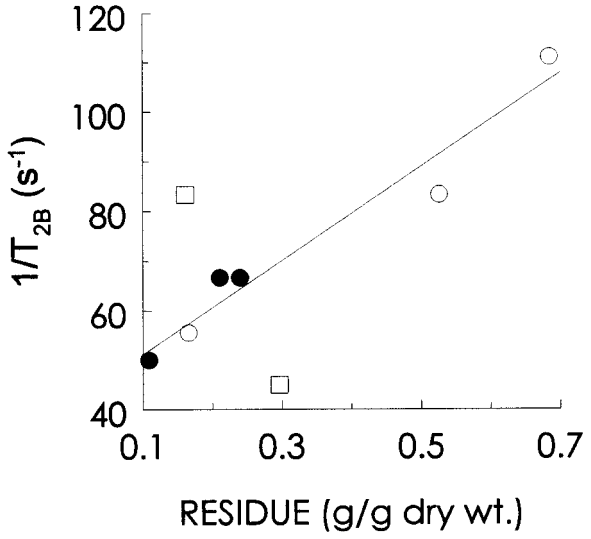


FIG. 8. The effect of residue concentration on the $T_2$ relaxation rate of component B of healthy (●,■) and degenerate (○,□) nucleus pulposus (●,○) and anulus fibrosus (■,□). The line of best fit for nucleus pulposus data is shown: $1/T_{2B} = 41.7 + 94.5$ RESIDUE. $R^2 = 0.95$; $P = 0.001$. Standard error of estimate = 5.6 $\text{sec}^{-1}$.

## DISCUSSION

### Relation to Other Studies

The qualitative agreement between the data obtained in this study and those reported in similar previous studies is strong. The relationships between water, collagen and, with the exception of Weidenbaum et al. (11), GAG concentrations agree (2,3) (Eq. [4]). Furthermore, the relationships between mean $1/T_2$ and both GAG and collagen concentrations also agree (6,7,11) (Eq. [13]; GAG data not shown). Thus, the trends in the data observed by this study are supported by the relevant literature. However, our conclusions differ from those of previous investigators because several additional aspects of the data have been considered, namely, the estimation of residue concentration, the consideration that the concentration of more than one component may contribute to the NMR results, the inclusion of the solid signal, and the recognition that relaxation rates increase with an increase in the concentration of chemical constituents.

Although the number of individual donors is relatively small, previously published studies relied on multiple samples from three (11) and four (6) specimens without distinguishing the relative effects of different donors and of

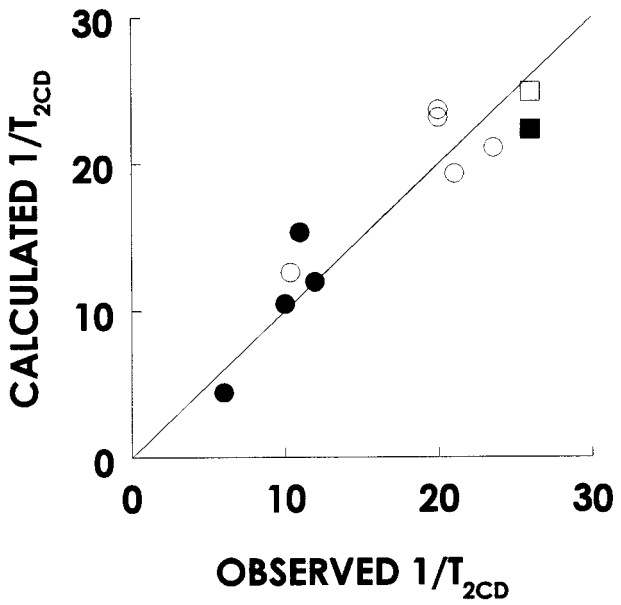


FIG. 9. The observed amplitude weighted mean relaxation rate of components C and D in healthy (●,■) and degenerate (○,□) nucleus pulposus (●,○) and anulus fibrosus (■,□) compared with values calculated from the equation $1/T_{2CD} = -11.3 + 41.4$ COLLAGEN + 36.7 RESIDUE. $R^2 = 0.86$; $P < 0.001$. Standard error of estimate = 3 $sec^{-1}$. The line represents equal observed and calculated values.

different samples from the same donor. Moreover, the correlations of strong statistical significance observed here lend credence to our conclusions. Additional specimens would seem unlikely to have added appreciable rigor.

### Residue

The chemical nature of the residue; that is, the noncollagen, non-GAG component of the dry weight, which averaged 0.34 g/g dry wt, is ill defined. The low molecular weight solutes of the interstitial fluid were calculated to be about 0.025 g/g dry wt. The concentration of elastin in disks is reported to be about 0.015 g/g dry wt (28). The protein core of the proteoglycan is about 10% of the weight of its GAG, or 0.030 g/g dry wt. Together, these three components represent about 20% of the total weight of the residue. The noncollagenous proteins of the disk have been estimated to be 0.20 to 0.45 g/g dry wt of NP and 0.05 to 0.25 g/g dry wt of AF (29). Histological studies of the disk also support the identification of the residue with the noncollagenous proteins. On examination by electron microscopy, the spaces between the collagenous fibers of both NP and AF are filled with granules believed to be proteins; the occasional collagenous fiber is covered with a thick sheath of such granules (30,31). Thus, the available data suggest that the noncollagenous proteins are the major constituents of the residue.

The residue was found to influence strongly the water concentration and NMR properties of the disk (Eqs. [4], [5], [7], [12], and [13]). The finding that the water content of the tissue decreased as the collagen increased (3,11) is explained by the observation that the concentration of water associated with collagen was less than that associated with GAG and residue (Eq. [4]).

### Solid and Mobile Components

In free-induction decay experiments, the fraction of solid tissue protons was close to the fraction of protons calculated to be present in collagen and the residue (Eq. [5]). This finding implies that the residue was either firmly attached to the collagen fiber meshwork or formed an independent solid component of the tissue. This conclusion is supported by the observation that 80% of tissue noncollagenous proteins were insoluble in 0.05M Na acetate buffer, pH 5.8, but were soluble in the same buffer containing 4M guanidinium chloride (32). The need to use acid hydrolysis to estimate the nitrogen concentration in the tissue (29) also supports this conclusion. In contrast, the fraction of mobile protons was close to the fraction of protons associated with water and GAG, as would be expected from the solubility of proteoglycan in the tissue water (Eq. [6]).

### $T_1$ and $T_2$ Relaxation Rates

Pure water has $T_1$ and $T_2$ relaxation times of about 3 sec. The observation of much shorter $T_1$ and $T_2$ relaxation times in disks reflects interactions between water and other tissue constituents. The observation of a primarily single exponential decay for $T_1$ indicates that all the water in disks diffuses sufficiently far, on the $T_1$ time scale of about 1 sec, that on average it experiences a homogeneous environment. Furthermore, magnetization exchange between nonaqueous and aqueous components of the disk was rapid on the $T_1$ time scale. On the shorter $T_2$ time scales, our measurements distinguished four distinct $T_2$ components. Therefore, at least for times of the order of 1–50 msec, water molecules experience a heterogeneous environment. If the diffusion coefficient for water were known, these time scales could be replaced by distance scales. Literature values of about $0.5–2 \times 10^{-5}$ $cm^2/sec$ for the water diffusion coefficient in disks (33) have been obtained at diffusion times of about 90 msec. Assuming that these diffusion coefficients are lower limits, the shorter $T_2$ components correspond to diffusion distances of 3–15 μm, distances corresponding reasonably with the dimensions of disk structures such as collagen fiber bundles. The longer time scale of $T_1$, over which the disk appears homogeneous to diffusing water molecules, corresponds to distance scales of about 100 μm. Restricted water diffusion or exchange between different water environments would blur these ranges.

The dependence of $1/T_1$ on collagen and residue (Eq. [7]) in disks suggests that GAG, which is undergoing considerable motion, has minimal effect upon the water relaxation rate in the disk. This conclusion is supported by the fact that the $1/T_1$ measured in viscous solutions of disk A1 proteoglycan were much smaller than those found when GAG was present at similar concentrations in the disk (Data not shown).

The bulk of the water in the NP, which contributed to the mean $T_2$ relaxation of components C and D, was associated with GAG and residue, while the smaller A and B components were associated with collagen (Fig. 7). The fraction of signal in $T_2$ component A could probably be assigned to water tightly associated with collagen fiber bundles. The proton fraction of component A corresponded to 0.3 g

water/g collagen. (NP water = 2.74 g/g dry wt; fraction of water protons in component A = 0.03; NP water in component A = 2.74 × 0.03 = 0.08 g/g dry wt; NP collagen = 0.31 g/g dry wt; NP water/g collagen = 0.08/0.31 = 0.3 g water/g collagen) A similar $T_2$ component (0.4 g/g collagen) was found in collagen from pig tendon (34).

### A Model of Disk Architecture

The NMR data can be summarized in a model that includes current knowledge of disk morphology and chemical constitution (Fig. 10). The $T_2$ relaxation rates suggest proton diffusion distances within water environments of the order of a few μm, distances resolvable by light microscopy. The $T_1$ data suggest further that the tissue should appear homogeneous on a scale of 100 μm, roughly the height of the outlines of the schematic in Fig. 10.

The free induction decay data indicated that the collagen of the tissue was solid (Eq. [5]). Since collagen molecules have a diameter of 1.5 nm, many such molecules would be present in the tissue structure of a few μm dimension responsible for $T_2$ component A. The location of this water must be within the interstices of the ordered bundles of collagen molecules (35,36). The three-fold larger pool of water associated with collagen concentration in $T_2$ component B seems likely to be located in the spaces between the collagenous fiber bundles, spaces that are less well ordered than the bundles themselves (cf. Eqs. [8] and [9]). Collagen comprises a much larger fraction of the tissue volume in the AF than in the NP, accounting for the larger contribution of $T_2$ components A and B to the relaxation rate of the AF relative to NP (Fig. 10).

The free induction decay experiments also identified the residue as a solid component of the disk (Eq. [5]). This observation suggests that the residue formed a space-occupying structure sterically excluding proteoglycans and sufficiently rigid to resist compression by the colloid osmotic pressure generated by the proteoglycans. The water in this compartment is responsible for the $T_2$ component C (Eq. [10] and Fig. 10). The remaining water, represented by component D, would contain the proteoglycans, the source of GAGs, the bulk of which are soluble in tissue water and would be distributed randomly in this space (Eq. [11] and Fig. 10). In the AF and degenerate NP, for which the signal from component D is not seen, the concentration of proteoglycan (GAG) is too low to form a distinct water compartment (Fig. 7).

## CONCLUSIONS

This study has demonstrated that the solid components of the disk are responsible for most of its NMR properties. To a large extent, the same relationships between NMR relaxation rates and chemical constitution hold for both NP and AF, suggesting that these two tissues represent a generalized disk structure comprising an insoluble meshwork of collagen and residue with an intercalated solution of proteoglycan. As disks degenerate, these same relationships are maintained. We expect that this work will help to increase specificity in the application of magnetic resonance techniques to the study of disk.

A work published since the submission of this article (37) presents data for 92 disks that support the relationships between $T_1$, $T_2$, water, GAG, and collagen described here. In healthy NP, $T_1$ and $T_2$ were positively correlated with water and GAG concentrations and negatively correlated with collagen concentration.

## ACKNOWLEDGMENTS

This research was supported by grants from the Natural Science and Engineering Research Council (ALM) and the Arthritis Society (RHP). The collection of specimens was assisted by the staff of the morgue at the Vancouver Hospital and Health Sciences Center. The NMR equipment was made available by Prof. Myer Bloom, Department of Physics. Dr. Mark E. Adams and Dr. Elliott Burnell undertook critical reviews of the manuscript.

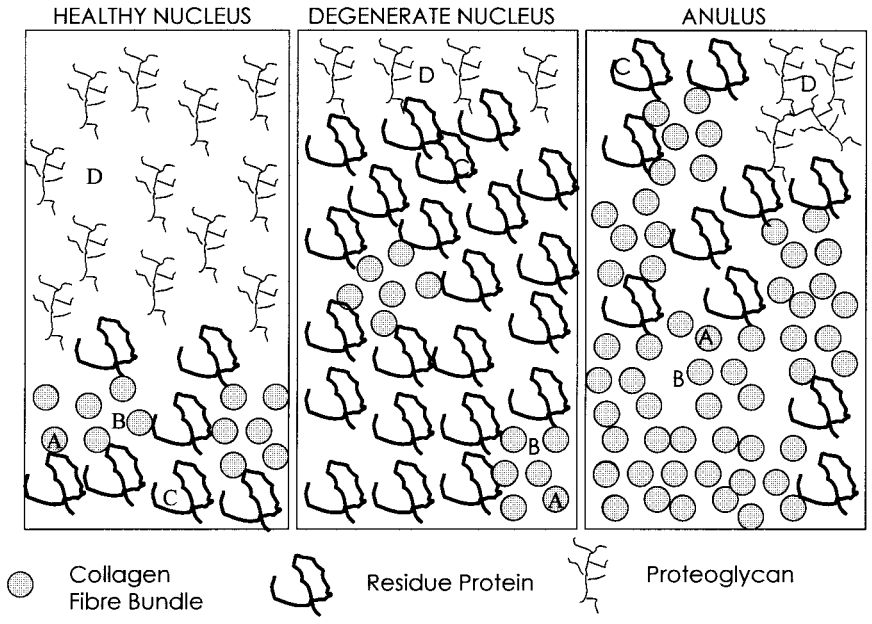


FIG. 10. A tentative model of disk architecture. The letters A, B, C, and D represent the suggested locations of the water protons associated with the corresponding $T_2$ components. The areas of each component in the schematic show roughly the fraction of tissue protons each represents.

## REFERENCES


1. Vernon-Roberts B. The normal aging of the spine: degeneration and arthritis. In: Andersson GBJ, McNeill TW, editors. Lumbar spinal stenosis. St. Louis, MO: Mosby; 1991. p 57–75.
2. Pearce RH. Chapter 27. Morphologic and chemical aspects of aging. In: Buckwalter JA, Goldberg VM, Woo SLY, editors. Musculoskeletal soft-tissue aging: impact on mobility. Rosemont, IL: American Academy of Orthopaedic Surgeons; 1993. p 363–379.
3. Antoniou J, Steffen T, Nelson F, Winterbottom N, Hollander AP, Poole AR, Aebi M, Alini M. The human lumbar intervertebral disc: evidence for changes in the biosynthesis and denaturation of the extracellular matrix with growth, maturation, ageing, and degeneration. J Clin Invest 1996;98:996–1003.
4. Modic MT. Chapter 3. Degenerative disorders of the spine. In: Modic MT, Masaryk TJ, Ross JS, editors. Magnetic resonance imaging of the spine. Second edition. St. Louis, MO: Mosby; 1994. p 80–149.
5. Gundry CR, Fritts HM. Magnetic resonance imaging of the musculoskeletal system. Part 8. The spine, section 1. Clin Orthop 1997;338:275–287.
6. Majors AW, MacDevitt CA, Silgalis I, Modic MT. A correlative analysis of T2, ADC and MT Ratio with water, hydroxyproline and GAG content in excised intervertebral disc. In: Proceedings of the 40th Annual Meeting, Orthopaedic Research Society, New Orleans, LA, 1994. p 116.
7. Antoniou J, Gouldsouzian NM, Heathfield TF, Pike B, Steffen T, Baramki HG, Poole AR, Alini M. Quantitative MR assessment of the human lumbar intervertebral disk related to matrix integrity and composition. In: Proceeding of the 42nd Annual Meeting, Orthopaedic Research Society, Atlanta, GA, 1996. p 679.
8. Chatani K, Kusaka Y, Mifune T, Nishikawa H. Topographic differences of 1H-NMR relaxation times (T1, T2) in the normal intervertebral disc and its relationship to water content. Spine 1993;18:2271–2275.
9. Yushmanov VY, Mitskevich VA. State of water in the intervertebral disks as shown by relaxational analysis of NMR tomograms. Biophysics 1989;34:926–929.
10. Ke JH, Zong LB, Natarajan RH, Andersson GBJ, Chen IH, Wang JZ, Turner DA. Relationship between MRI relaxation times and water content in intervertebral discs. In: Proceedings of the 39th Annual Meeting, Orthopaedic Research Society, San Francisco, CA, 1993. p 415.
11. Weidenbaum M, Foster RJ, Best BA, Nickoloff E, Newhouse J, Ratcliffe A, Mow VC. Correlating magnetic resonance imaging with the biochemical content of the normal human intervertebral disc. J Orthop Res 1992;10:552–561.
12. Chiu EJ, Hewitt DC, Hu SS, Lotz JC, Majumdar S. Correlation of MR-derived diffusion coefficients and relaxation times with intervertebral disc tissue hydration in vitro. In: Proceedings of the Fifth Scientific Meeting, International Society for Magnetic Resonance in Medicine, Vancouver, BC, Canada, 1997. p 144.
13. Eyre D, Benya P, Buckwalter J, Caterson B, Heinegard D, Pearce R, Pope M, Urban J. Chapter Five. Intervertebral Disk. Part B. Basic Science Perspectives. In: Frymoyer JW, Gordon SL, Editors. New perspectives on low back pain. Park Ridge, IL: American Academy of Orthopaedic Surgeons; 1989. p 147–207.
14. Sternin E. Data acquisition and processing: a systems approach. Rev Sci Instrum 1985;56:2043–2049.
15. Abragam A. Principles of magnetic resonance. Oxford, UK: Oxford University; 1961.
16. Carr HY, Purcell EM. Effects of diffusion on free precession in nuclear magnetic resonance experiments. Phys Rev Section H 1954;94:630–638.
17. Meiboom S, Gill D. Modified spin echo method for measuring nuclear relaxation times. Rev Sci Instrum 1958;29:688–691.
18. Whittall KP, MacKay AL. Quantitative interpretation of NMR relaxation data. J Magn Reson 1989;84:134–152.
19. Pearce RH, Grimmer BJ, Adams ME. Degeneration and the chemical composition of the human lumbar intervertebral disc. J Orthop Res 1987;5:198–205.
20. Woessner JF Jr. The determination of hydroxyproline in tissue and protein samples containing small proportions of this imino acid. Arch Biochem Biophys 1961;93:440–447.
21. Bebault GM, Pearce RH. Assay of keratan sulfate as anion-exchanger bound hexose. Connect Tissue Res 1991;25:281–293.
22. Johnstone B, Urban JPG, Roberts S, Menage J. The fluid content of the human intervertebral disc. Comparisons between fluid content and swelling pressure profiles of discs removed at surgery and those taken postmortem. Spine 1992;17:412–416.
23. Tengblad A, Pearce R H, Grimmer B J. Demonstration of link protein in proteoglycan aggregates from human intervertebral disc. Biochem J 1984;222:85–92.
24. Zimmerman JR, Brittin WE. Nuclear magnetic resonance studies in multiple phase systems: lifetime of a water molecule in an absorbing phase on silica gel. J Phys Chem 1957;61:1328–1333.
25. Herbert CM, Lindberg KA, Jayson MIV. Changes in the collagen of human intervertebral discs during aging and degenerative disk disease. J Mol Med 1975;1:75–91.
26. Creighton TE. Proteins. Structures and molecular properties. 2nd edition. New York: Freeman; 1993.
27. Urban JPG, Maroudas A. The measurement of fixed charge density in the intervertebral disc. Biochim Biophys Acta 1979;586:166–178.
28. Olczyk K. Changes in macromolecular components of prolapsed intervertebral discs. Ann Biol Clin (Paris) 1994;52:711–716.
29. Dickson IR, Happey F, Pearson CH, Naylor A, Turner RL. Variations in the protein components of human intervertebral disk with age. Nature 1967;215:50–53.
30. Buckwalter JA. The fine structure of human intervertebral disc. In: White AA III, Gordon SL, editors. Symposium on idiopathic low back pain. St. Louis, MO: Mosby; 1982. p 108–143.
31. Buckwalter JA, Maynard JA, Cooper RR. Sheathing of collagen fibrils in human intervertebral disc. J Anat 1978;125:615–618.
32. Sorce D, McDevitt CA, Green W, Greenwald RA, Moak S. Non-collagenous proteins of the human nucleus pulposus. In: Proceedings of the 30th Annual Meeting, Orthopaedic Research Society, Atlanta, GA, 1984. p 282.
33. Chiu EJ, Hewitt DC, Hu SS, Lotz JC, Majumadar S. MRI measurement of water diffusion in the human intervertebral disc with compression. In: Proceedings of the 43rd Annual Meeting, Orthopaedic Research Society, San Francisco, CA, 1997. p 123.
34. Peto S, Gillis P. Fiber-to-field angle dependence of proton nuclear magnetic relaxation in collagen. Magn Reson Imaging 1990;8:705–712.
35. Piez KA. Molecular and aggregate structures of the collagens. In: Piez KA, Reddi AH, editors. Extracellular matrix biochemistry. New York, NY: Elsevier; 1984. p 1–39.
36. Bateman JF, Lamande SR, Ramshaw JAM. Collagen superfamily. In: Comper WD, editor. Extracellular matrix. Volume 2. Molecular components and interactions. Amsterdam: Harwood; 1996. p 22–67.
37. Antoniou J, Pike GB, Steffen T, Baramki H, Poole AR, Aebi M, Alini M. Quantitative magnetic resonance imaging in the assessment of degenerative disc disease. Magn Reson Med 1998;40:900–907.